J|A|C|S
ARTICLES
Published on Web 09/03/2003

Low-Temperature NMR Studies of the Structure and Dynamics of a Novel Series of Acid−Base Complexes of HF with Collidine Exhibiting Scalar Couplings Across Hydrogen Bonds†

Ilja G. Shenderovich,[‡,§] Peter M. Tolstoy,[‡,§] Nikolai S. Golubev,*[,§] Sergei N. Smirnov,[§] Gleb S. Denisov,[§] and Hans-Heinrich Limbach*[,‡]

Contribution from the Institut für Chemie der Freien Universität Berlin, Takustrasse 3, D-14195 Berlin, Germany and Institute of Physics, St. Petersburg State University, 198504 St. Petersburg, Russian Federation

Received November 1, 2002; E-mail: limbach@chemie.fu-berlin.de; Nick.Golubev@pobox.spbu.ru

Abstract: The low-temperature ^{1}H, ^{19}F, and ^{15}N NMR spectra of mixtures of collidine-^{15}N (2,4,6-trimethylpyridine-^{15}N, Col) with HF have been measured using CDF_3/CDF_2Cl as a solvent in the temperature range 94−170 K. Below 140 K, the slow proton and hydrogen bond exchange regime is reached where four hydrogen-bonded complexes between collidine and HF with the compositions 1:1, 2:3, 1:2, and 1:3 could be observed and assigned. For these complexes, chemical shifts and scalar coupling constants across the $^{19}F^{1}H^{19}F$ and $^{19}F^{1}H^{15}N$ hydrogen bridges have been measured which allowed us to determine the chemical composition of the complexes. The simplest complex, collidine hydrofluoride ColHF, is characterized at low temperatures by a structure intermediate between a molecular and a zwitterionic complex. Its NMR parameters depend strongly on temperature and the polarity of the solvent. The 2:3 complex $[ColHFHCol]^+[FHF]^-$ is a contact ion pair. Collidinium hydrogen difluoride $[ColH]^+[FHF]^-$ is an ionic salt exhibiting a strong hydrogen bond between collidinium and the $[FHF]^-$ anion. In this complex, the anion $[FHF]^-$ is subject to a fast reorientation rendering both fluorine atoms equivalent in the NMR time scale with an activation energy of about 5 kcal mol^{-1} for the reorientation. Finally, collidinium dihydrogen trifluoride $[ColH]^+[F(HF)_2]^-$ is an ionic pair exhibiting one FHN and two FHF hydrogen bonds. Together with the $[F(HF)_n]^-$ clusters studied previously (Shenderovich et al., *Phys. Chem. Chem. Phys.* **2002**, *4*, 5488), the new complexes represent an interesting model system where the evolution of scalar couplings between the heavy atoms and between the proton and the heavy atoms of hydrogen bonds can be studied. As in the related FHF case, we observe also for the FHN case a sign change of the coupling constant $^{1}J_{FH}$ when the F···H distance is increased and the proton shifted to nitrogen. When the sign change occurs, that is, $^{1}J_{FH} = 0$, the heavy atom coupling constant $^{2}J_{FN}$ remains very large, of the order of 95 Hz. Using the valence bond order model and hydrogen bond correlations, we describe the dependence of the hydrogen bond coupling constants, of hydrogen bond chemical shifts, and of some H/D isotope effects on the latter as a function of the hydrogen bond geometries.

Introduction

In aprotic solvents or proteins, acids AH and bases B can form a number of different hydrogen bonded complexes, for example $(AH)_nB$,[1] $[AHA]^-$ or $[BHB]^+$,[2,3] which can exhibit a multitude of protonation states or hydrogen bond geometries. By contrast, in aqueous solution, AH and B are separated, hydrogen bonded to water molecules, and can each exhibit only two protonation states. Unfortunately, the study of the hydrogen bond geometries in a series of complexes of the type $(AH)_nB$ is experimentally very difficult. In the solid state, several complexes of pyridine with a varying number of HF molecules have been described.[4] In this series, with increasing *n*, the proton of the F−H···N hydrogen bond was gradually shifted from F toward the hydrogen bond center, accompanied by a shortening of the F···N distance. A similar phenomenon was observed recently in a series of 1:1 complexes of collidine with carboxylic

† Presented at the 101. Annual Meeting of the Deutsche Bunsengesellschaft für Physikalische Chemie on "Kern und Elektronenspins als dynamische und kinetische Sonden", Potsdam, Germany, 9.5.-11.5.2002.

‡ Institut für Chemie der Freien Universität Berlin.

§ St. Petersburg State University.

(1) (a) Davis, M. M. *Acid−Base Behavior in Aprotic Organic Solvents*, *Natl. Bur. Standards Monograph* **1968**, *105*, 1. (b) Zeegers-Huyskens, Th.; Sobczyk, L. *J. Mol. Liq.* **1990**, *46*, 263. (c) Schreiber, V. M.; Kulbida, A. I.; Rospenk, M.; Sobczyk, L.; Rabold, A.; Zundel, G. *J. Chem. Soc., Faraday Trans.* **1996**, *92*, 2555. (d) Barnes, A. J.; Larsson, E.; Nielsen, C. J. *J. Mol. Struct.* **1994**, *322*, 165. (e) Borisenko, V. E.; Denisov, G. S.; Zavjalova, Y. A.; Furin, G. G. *J. Mol. Struct.* **1994**, *322*, 151.

(2) (a) Golubev, N. S.; Denisov, G. S. *J. Mol. Struct.* **1992**, *270*, 263. (b) Ilczyszyn, M.; Ratajczak, H. *J. Chem. Soc., Faraday Trans.* **1995**, *91*, 1611; ibid. **1995**, *91*, 3859. (c) Szafran, M. *J. Mol. Struct.* **1996**, *381*, 39.

(3) Schah-Mohammedi, P.; Shenderovich, I. G.; Detering, C.; Limbach, H. H.; Tolstoy, P. M.; Smirnov, S. N.; Denisov, G. S.; Golubev, N. S. *J. Am. Chem. Soc.* **2000**, *122*, 12878.

(4) (a) Gennick, I.; Harmon, K. M.; Potvin, M. M. *Inorg. Chem.* **1976**, *16*, 2033. (b) Boenigk, D.; Mootz, D. *J. Am. Chem. Soc.* **1988**, *110*, 2135.

10.1021/ja029183a CCC: $25.00

acids of increasing acidity using X-ray[5a] and solid-state NMR.[5b] On the other hand, when a 1:1 crystalline acid−base complex is dissolved in an aprotic solvent, a mixture of several complexes usually is formed which makes it difficult to assign their individual spectroscopic features such as vibrational bands and NMR signals. The NMR problem has been overcome in the past years with the synthesis and use of CDF_3/CDF_2Cl Freon mixtures which allow one to reach the slow proton and hydrogen bond exchange regime between 95 and 150 K.[3,6,7] The polarity of these solvents strongly increases when temperature is lowered.[8,9] Using this technique, various hydrogen bonded species of pyridine with various acids[6a,6b] and of fluoride with HF[6d,f] have been characterized. Especially the latter series has obtained much attention because a novel property of strong hydrogen bonds was observed, that is, spin−spin couplings between heavy atoms and between H and an heavy atom across a hydrogen bond.[6d] The two-bond spin coupling constant, $^2J_{FF}$, decreased rapidly with an increase of the F···F distance, which is itself affected by deuteration.[6f] Moreover, $^2J_{FF}$ was found to be larger than the coupling constant $^1J_{HF}$ across the hydrogen bond at large H···F distances. This fact arises from a sign change of $^1J_{HF}$ when this distance is increased. The effect was modeled by DFT ab initio calculations[6e] and reproduced by accurate ab initio CCSD calculations.[10] Scalar couplings have been observed recently across NHN hydrogen bonds of molecules of biological interest[11] and are studied intensively by ab initio calculations.[12] Again, a sign change of $^1J_{HN}$ was observed when the H···N distance was increased.[11d]

In a recent paper,[13] we have reported the multinuclear NMR spectra of the 1:1 complex collidine−HF (ColHF) dissolved in CDF_3/CDF_2Cl, exhibiting an extremely strong low-barrier hydrogen bond. An enormous two-bond spin coupling constant was found, $^2J_{FN} = 96$ Hz, which did not change much with temperature. On the other hand, $^1J_{FH}$ decreased strongly and almost vanished when temperature was decreased. This effect was tentatively attributed again to a sign change of $^1J_{FH}$ with increasing F···H distance caused by the increase of the solvent polarity at low temperatures which shifts the mean proton location from F toward N. This interpretation was corroborated by the observation of H/D isotope effects on the chemical shifts.[8] If this interpretation was true, we expected that $^1J_{FH}$ would be again observable when the F···H distance is further increased. We tried, therefore, to reach this regime by addition of further FH molecules to the ColHF complex, leading to $Col(HF)_2$ and $Col(HF)_3$. This strategy succeeded as shown by a series of low-temperature multinuclear NMR experiments of collidine−$(HF)_n$ mixtures in CDF_3/CDF_2Cl described in this paper. We observed in addition also the complex $[ColHFHCol]^+$; the remaining complex, that is, the homoconjugate cation $[ColHCol]^+$, had been observed previously.[3] In the following, after the Experimental Section, the results of the experiments are described and discussed.

Experimental Section

Materials. As a low-temperature NMR solvent, a mixture of two Freons, CDF_3/CDF_2Cl exhibiting the freezing point below 100 K was prepared as reported previously.[6a,8] Collidine, enriched with ^{15}N to about 96%, was synthesized from trimethylpyrilium tetrafluoroborate and ammonium chloride-^{15}N as described before.[6c] The NMR samples were prepared as follows. Calculated amounts of collidine in dichloromethane and of hydrofluoric acid (48% aqueous solution, Aldrich) were placed into a Teflon flask. Then, water was removed by azeotropic distillation with dichloromethane. When the resulting oils were kept at −20 °C, crystalline products were obtained. The low-temperature NMR spectra of these products dissolved in the above-mentioned Freon mixture showed a superposition of various complexes. Therefore, no attempts were made to isolate and characterize the crystalline salts, and for the measurements described below, the oily mixtures were placed in an NMR glass tube equipped with a Teflon needle valve (Wilmad, Buena, USA) for vacuum operations, resisting a pressure up to 50 bar. The tube was then connected to a vacuum line, and the solvent was added by vacuum transfer.

NMR Spectra. The NMR spectra were recorded on a Bruker AMX-500 instrument equipped with a special probe head allowing measurements down to 90 K. The ^1H and ^{19}F chemical shifts were measured using the CHF_3 peaks as internal references and then converted into the usual scales corresponding to TMS and $CFCl_3$. The ^{15}N chemical shifts were referenced to the peak of free collidine. These data can be converted into the solid $^{15}NH_4Cl$ scale where $\delta(^{15}N\text{-Col}) = 268$ ppm.

To extract rate constants from temperature-dependent line shapes of the $Col(HF)_2$ complex, we used a homemade computer program based on the procedure DNMR2 of Binsch et al.[14] The system was treated as a system of five spins, with a mutual exchange of the two fluorines. The spectra were characterized by the chemical shifts, coupling constants, and the effective transverse relaxation times $T_{2i} = 1/\pi W_{oi}$ of each individual transition i.

Results

The results of all measurements are assembled in Table 1. Figure 1 gives an overview over the low-temperature ^1H NMR spectra of solutions of collidine and HF, where the HF/collidine ratio increases from the top to the bottom. The spectra show major spectral changes arising from the formation of various complexes assigned to the structures depicted in Figure 1. These

(5) (a) Foces-Foces, C.; Llamas-Saiz, A. L.; Lorente, P.; Golubev, N. S.; Limbach, H. H. *Acta Crystallogr.* **1999**, *C55*, 377. (b) Lorente, P.; Shenderovich, I. G.; Buntkowsky, G.; Golubev, N. S.; Denisov, G. S.; Limbach, H. H. *Magn. Reson. Chem.* **2001**, *39*, S18.
(6) (a) Golubev, N. S.; Smirnov, S. N.; Gindin, V. A.; Denisov, G. S.; Benedict, H.; Limbach, H. H. *J. Am. Chem. Soc.* **1994**, *116*, 12055. (b) Smirnov, S. N.; Golubev, N. S.; Denisov, G. S.; Benedict, H.; Schah-Mohammedi, P.; Limbach, H. H. *J. Am. Chem. Soc.* **1996**, *118*, 4094. (c) Golubev, N. S.; Smirnov, S. N.; Schah-Mohammedi, P.; Shenderovich, I. G.; Denisov, G. S.; Gindin, V. A.; Limbach, H. H. *Russian J. Gen. Chem.* **1997**, *67*, 1150. (d) Shenderovich, I. G.; Smirnov, S. N.; Denisov, G. S.; Gindin, V. A.; Golubev, N. S.; Dunger, A.; Reibke, R.; Kirpekar, S.; Malkina, O. L.; Limbach, H. H. *Ber. Bunsen-Ges. Phys. Chem.* **1998**, *102*, 422. (e) Benedict, H.; Shenderovich, I. G.; Malkina, O. L.; Malkin, V. G.; Denisov, G. S.; Golubev, N. S.; Limbach, H. H. *J. Am. Chem. Soc.* **2000**, *122*, 1979. (f) Shenderovich, I. G.; Limbach, H. H.; Smirnov, S. N.; Tolstoy, P. M.; Denisov, G. S.; Golubev, N. S. *Phys. Chem. Chem. Phys.* **2002**, *4*, 5488. (g) Smirnov, S. N.; Benedict, H.; Golubev, N. S.; Denisov, G. S.; Kreevoy, M. M.; Schowen, R. L.; Limbach, H. H. *Can. J. Chem.* **1999**, *77*, 943.
(7) Denisov, G. S.; Bureiko, S. F.; Golubev, N. S.; Tokhadze, K. G. In *Molecular Interactions*, Ratajczak, H.; Orville-Thomas, W. J., Eds.; John Wiley & Sons: Chichester − New York − Brisbane − Toronto, 1981; Vol. 2, p 107.
(8) Shenderovich, I. G.; Burtsev, A. P.; Denisov, G. S.; Golubev, N. S.; Limbach, H. H. *Magn. Res. Chem.* **2001**, *39*, S91.
(9) Golubev, N. S.; Denisov, G. S.; Smirnov, S. N.; Shchepkin, D. N.; Limbach, H. H. *Z. Phys. Chem. (Muenchen)* **1996**, *196*, 73.
(10) Perera, S. A.; Bartlett, R. J. *J. Am. Chem. Soc.* **2000**, *122*, 1231.
(11) (a) Dingley, A. J.; Grzesiek, S. *J. Am. Chem. Soc.* **1998**, *120*, 8293. (b) Cornilescu, G.; Ramirez, B. E.; Frank, M. K.; Clore, G. M.; Gronenborn, A. M.; Bax, A. *J. Am. Chem. Soc.* **1999**, *121*, 6275. (c) Pervushin, K.; Ono, A.; Fernández, C.; Szyperski, T.; Kainosho, M.; Wütrich, K. *Proc. Natl. Acad. Sci. U.S.A.* **1998**, *95*, 14147. (d) Pietrzak, M.; Limbach, H. H.; Perez-Torralba, M.; Sanz, D.; Claramunt, R. M.; Elguero, J. *Magn. Reson. Chem.* **2001**, *39*, S100.
(12) (a) Del Bene, J. E.; Bartlett, R. J. *J. Am. Chem. Soc.* **2000**, *112*, 10480. (b) Del Bene, J. E.; Perera, S. A.; Bartlett, R. J. *Magn. Reson. Chem.* **2001**, *39*, S109.
(13) Golubev, N. S.; Shenderovich, I. G.; Smirnov, S. N.; Denisov, G. S.; Limbach, H. H. *Chem.−Eur. J.* **1999**, *5*, 492.
(14) (a) Binsch, G. *J. Am. Chem. Soc.* **1969**, *91*, 1304. (b) Binsch, G.; Kleier, D. A. *Quantum Chemistry Program Exchange*; Indiana University: Bloomington, IN; #140, http://qcpe.chem.indiana.edu/.

Table 1. Parameters of the FHF and NHF Hydrogen Bonds of $[F(HF)_n]^-$ and Col$(HF)_n$ Clusters in CDF_3/CDF_2Cl

species	BHA	$^1J_{BH}$/Hz	$^1J_{HA}$/Hz	$^2J_{AB}$/Hz	δ_H/ppm	δ_B/ppm	δ_A/ppm	T/K[a]	r_{BH}/Å	r_{HA}/Å	q_1/Å	q_2/Å
FHF^-	FHF	124	124	220	16.60	−155.4	−	130	1.148	1.148	0	2.299
$F^-(HF)_2$	FHF	−24.5	354	146.5	14.015	−148.75	−176.9	130	1.349	1.012	0.169	2.361
$F^-(HF)_3$	FHF	−45	430	94	11.79	−147.08	−185.5	130	1.451	0.979	0.236	2.430
$F^-(HF)_4$	FHF		483		10.2		−191.4	130	1.540	0.961	0.290	2.501
ColHFHF	FHF	<10	280	155	15.76	−126.2	−166.2	97	1.30	1.04	−0.13	2.34
Col$HF(HF)_2$	FHF	−38	400	99	12.9	−131	−180.3	130	1.46	0.98	−0.24	2.44
ColHF	NHF	−39	88		19.4		−121.5	180	1.24	1.17	−0.04	2.41
ColHF	NHF	−42	75	−96	19.6		−118.5	170	1.23	1.18	−0.03	2.41
ColHF	NHF	−43	66	−96	19.6		−118.05	170	1.22	1.18	−0.02	2.41
ColHF	NHF	−45	37	−96	19.95	−63.47		155	1.20	1.21	0.01	2.41
ColHF	NHF	−45	45	−96	19.88		−114.9	150	1.21	1.20	0	2.41
ColHF	NHF	−48	34	−96	19.97		−114.18	145	1.20	1.21	0.01	2.41
ColHF	NHF	−50	25		20.02			145	1.19	1.22	0.02	2.42
ColHF	NHF	−50	22		19.98			135	1.19	1.23	0.02	2.42
ColHF	NHF	−51	15	−96	20.10	−67.27	−111.5	130	1.18	1.24	0.03	2.42
ColHF	NHF	−48	14		20.02			125	1.18	1.24	0.03	2.42
ColHF	NHF	−50			20.08			125	1.16	1.27	0.05	2.43
ColHF	NHF	−51			20.09		−110.34	125	1.16	1.28	0.06	2.43
ColHF	NHF	−55			20.12			112	1.15	1.29	0.07	2.44
ColHF	NHF	−		−96	20.22		−107.8	103	1.14	1.31	0.08	2.45
ColHFHCol	NHF	−75	−71	−64	18.4	−88.4	−89.2	120	1.08	1.46	0.19	2.54
ColHFHF	NHF	−86	−75		16.69	−94.4		120	1.05	1.61	0.28	2.66
Col$HF(HF)_2$	NHF	−90	−45		15.09	−97.8	−131	130	1.02	1.85	0.42	2.87
Col$HF(HF)_3$	NHF	−92			14.02	−105.7		130				−

[a] Dielectric constant of the CDF_3/CDF_2Cl mixture is a function of temperature and solvent composition. [b] Chemical shifts are measured with respect to TMS (^{1}H), CDF_3 (^{19}F, converted into the $CFCl_3$ scale), and free collidine (^{15}N, corresponds to 268 ppm in the solid $^{15}NH_4Cl$ scale) as internal standards.

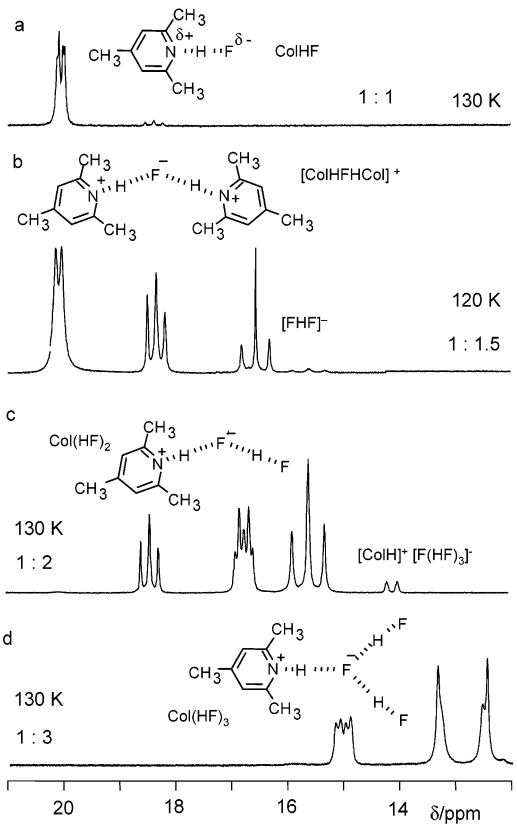

Figure 1. ^{1}H NMR signals of the hydrogen bond protons of various complexes between collidine-^{15}N and HF in CDF_3/CDF_2Cl. From parts a−d, the concentration of HF is increased.

structures were confirmed by additional ^{19}F and ^{15}N experiments described below. We observe almost in all cases first-order splitting patterns; however, the individual lines of a given pattern exhibit often differential line widths. The phenomenon of differential line widths of scalar coupled NMR transitions is well-known[6d,15] and can be used to determine the sign of coupling constants. For example, Shimidzu determined the sign of the coupling constant $^2J_{HF}$ in $CHFCl_2$.[15a] The theory of this effect has been reviewed recently.[16] It occurs when the inverse correlation time of the molecular reorientation is of the order of the Larmor frequency and when two relaxation mechanisms with a common correlation time interfere, for example, dipolar−dipolar or dipolar−chemical shift anisotropy (CSA) relaxation mechanisms. The increase of the correlation time is caused here by the increase of the solvent viscosity at low temperatures. A detailed discussion of how the signs of the couplings are determined will be given below.

1:1 Collidine−HF Complex ColHF. In Figure 2 are depicted the multinuclear temperature-dependent signals of a collidine−HF solution, containing an excess of the base. These spectra have been reported previously;[13] we need to repeat their description here for a better understanding of the spectral changes at higher HF/collidine ratios.

At 200 K, the ^{1}H spectrum (Figure 2a) exhibits an exchange broadened doublet around 18.2 ppm. When temperature is lowered, the signal is shifted to low field and narrows into a doublet of doublets by coupling with ^{19}F and ^{15}N. The larger coupling is determined by $^1J_{HF}$, and the smaller, by $^1J_{NH}$. The absolute value of $^1J_{HF}$ decreases and that of $^1J_{NH}$ increases when temperature is lowered; they are equal around 150 K giving rise to a triplet. Around 110 K, $^1J_{HF}$ is smaller than the line width of 10 Hz and is no longer resolved.

In Figure 2b are depicted the corresponding changes of the fluorine signal. At the higher temperatures, it consists also of a doublet of doublets arising from couplings with ^{1}H and ^{15}N.

(15) (a) Shimidzu, H. *J. Chem. Phys.* **1964**, *40*, 3357. (b) Rüterjans, H.; Kaun, E.; Hull, W. E.; Limbach, H. H. *Nucleic Acids Res.* **1982**, *10*, 7027. (c) Griffey, R. H.; Poulter, C. D.; Yamaizumi, Z.; Nishimura, S.; Hurd, R. E. *J. Am. Chem. Soc.* **1982**, *104*, 5811. (d) Gueron, M.; Leroy, J. L.; Griffey, R. H. *J. Am. Chem. Soc.* **1983**, *105*, 7262. (e) Farrar, T. C.; Adams, B. R.; Grey, G. C.; Quintero-Arcaya, R. A.; Zuo, Q. *J. Am. Chem. Soc.* **1986**, *108*, 8190.

(16) Kumar, A.; Christy Rani Grace, R.; Madhu, P. K. *Cross-correlations in NMR* in *Prog. in NMR Spectroscopy* **2000**, *37*, 191.

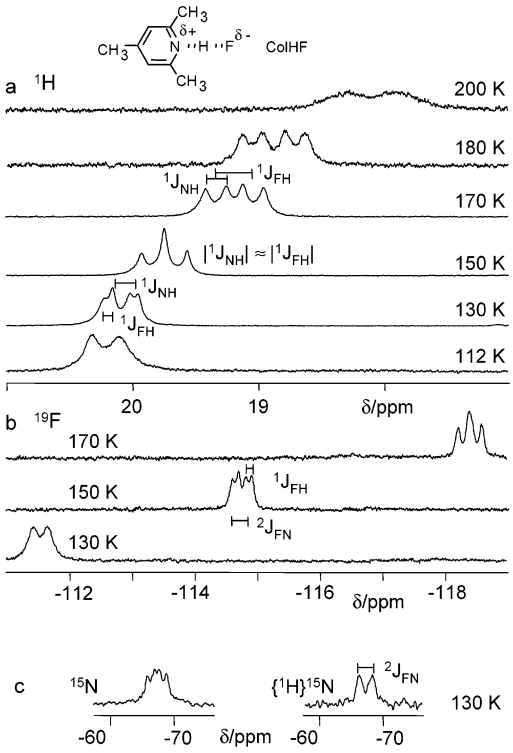

Figure 2. (a) ^{1}H NMR signals of the hydrogen bond proton of the 1:1 complex between collidine-^{15}N and HF in CDF_3/CDF_2Cl of a sample containing a 10-fold excess of collidine. (b) ^{19}F NMR spectra of the same sample. (c) ^{15}N spectra with and without proton decoupling at 130 K of a sample containing a 7-fold excess of collidine. In this sample, additional hydrogen bonded complexes are observed by ^{1}H NMR. Adapted from ref 13.

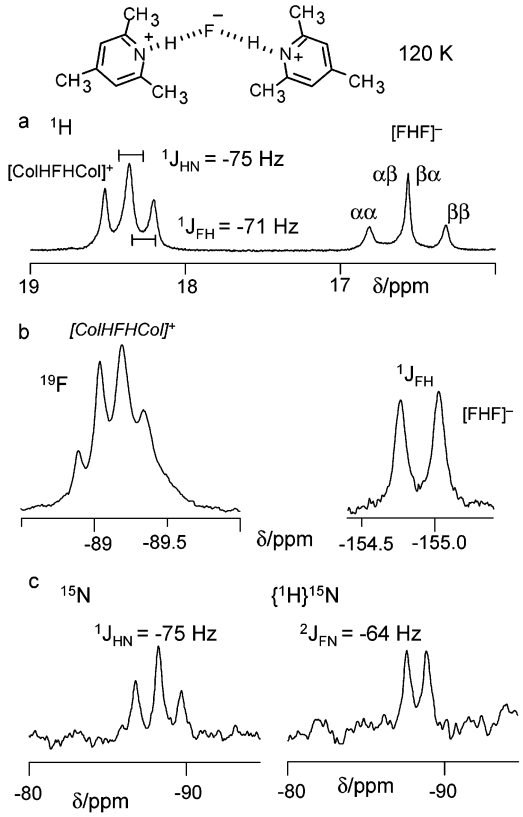

Figure 3. Low-temperature ^{1}H (a), ^{19}F (b), and ^{15}N (c) signals of $[ColHFHCol]^+[FHF]^-$ in CDF_3/CDF_2Cl at 120 K.

Again, $^1J_{HF}$ decreases and is no longer resolved at low temperatures. By contrast, the coupling $^2J_{FN} = 96$ Hz across the hydrogen bond remains fairly constant in the temperature range covered.

The ^{15}N signal at 130 K is shifted by −67 ppm to high field with respect to the separate signal of free collidine absorbing at 268 ppm referenced to solid ammonium chloride[6c] (Figure 2c). Again, the expected doublet of doublets is observed arising from coupling with ^{1}H and ^{19}F. By ^{1}H decoupling, $^1J_{NH}$ is removed and a doublet remains characterized by $^2J_{FN}$.

The signs of the coupling constants listed in Table 1 are determined by analysis of the differential line width. As discussed previously,[6d,f] the triplet of FHF^- (see an example later in Figure 3a) exhibits two broad outer components, associated to the fluorine spin states αα and ββ. The H-bond proton experiences the added dipolar coupling of both fluorines leading to an enhanced transverse relaxation time, that is, line broadening of these components.[6d,f] The central component is associated with the fluorine spin states αβ and βα. As FHF^- is linear, the two dipolar H···F couplings cancel each other, and hence the line width is smaller as compared to the outer components. In other words, there is an interference between the F···H and the H···F dipolar relaxation mechanisms. According to the theory of the three spin system,[17] this means that the sign of $^1J_{HF}$ is positive, which is in agreement with theoretical calculations.[6d,10] Furthermore, we note that the broad high-field component is a little bit narrower than the broad low-field component. This effect arises from an interference of the dipolar with the CSA relaxation mechanism, a positive coupling constant $^1J_{HF}$ and an axially symmetric ^{1}H CSA tensor with $\sigma_{||} - \sigma_{\perp} \rightarrow 0$.[15e] A substantial differential line width, that is, a broader low-field and a narrower high-field component are observed in the signals of ColHF around 130 K (Figure 2a), indicating that $^1J_{HF}$ is still positive. As dipolar relaxation by ^{15}N is less effective than by ^{19}F, the differential line widths of the doublet components arising from coupling with ^{15}N are less pronounced. However, large ^{1}H−^{15}N couplings are always negative, where the sign is caused by the negative gyromagnetic ratio of ^{15}N.

The sign of $^2J_{FN}$ could not be determined by a differential line width analysis. However, up to date no negative coupling constants across hydrogen bonds between heavy atom nuclei exhibiting the same sign of the gyromagnetic ratio have been observed. Therefore, we can safely assume that $^2J_{FN}$ is negative because of the negative gyromagnetic ratio of ^{15}N. As a consequence, for the remaining complexes described in the following, which exhibit fairly large ^{1}H−^{15}N couplings, we assume that the signs of $^2J_{FN}$ and $^1J_{HN}$ remain negative.

2:3 Collidine−HF Complex $[ColHFHCol]^+[FHF]^-$. In Figure 3 are depicted the signals of the species which dominate at a base−acid ratio of 2:3. We assign this complex to the ionic pair $[ColHFHCol]^+[FHF]^-$. This salt contributes two triplets of equal intensities in the hydrogen bond region (Figure 3a). The triplet at $\delta = 16.6$ ppm discussed already above is typical for $[FHF]^-$, characterized by a coupling to fluorine of $^1J_{FH} = 124$ Hz.[3,6d,18] In the fluorine spectrum, a corresponding doublet exhibiting the same splitting is observed at −154.9 ppm. The

(17) Emsley, J. W.; Feeney, J.; Sutcliffe, L. H. *High-Resolution Nuclear Magnetic Resonance Spectroscopy*; Pergamon Press: Oxford, 1965; Vol. 1.

signal at $\delta = 18.4$ ppm has the appearance of a triplet, but it corresponds in reality to a nonresolved doublet of doublets, with $^1J_{NH} = -75$ Hz and $|^1J_{FH}| = 71$ Hz. This interpretation is corroborated by the analysis of the ^{15}N signal, exhibiting an NF doublet splitting of $^2J_{NF} = -64$ Hz after ^1H decoupling, and an additional doublet splitting of $^1J_{HN} = -75$ Hz (Figure 3c). Finally, the second fluorine signal at -89.2 ppm corresponds to a triplet of triplets, arising from coupling with the two bridging protons and the two nitrogen nuclei. Similar values of the $^1J_{FH}$ and $^2J_{NF}$ constants lead to an apparent pentet structure.

It is interesting to compare the differential line widths of the transitions arising from the $^1H-^{19}F$ coupling in the ^1H and the ^{19}F signals of the NHF−hydrogen bond of ColHF (Figure 2) with the corresponding line widths of $[ColHFHCol]^+$ (Figure 3). In the former, the low-field components are broader than the high-field components, whereas the opposite is true for $[ColHFHCol]^+$. The effect is particularly well demonstrated by comparison of the quasi-triplets in Figure 2a at 130 K and in Figure 3a and by comparison of the ^{19}F signals in Figure 2b at 150 K and in Figure 3b. Assuming that the CSA tensors did not change sign, this finding means that the sign of the $^1H-^{19}F$ coupling has changed, that is, that $^1J_{FH} = -71$ Hz for $[ColHFHCol]^+$.

1:2 Collidine−HF Complex $[ColH]^+[FHF]^-$. At a 1:2 base−acid ratio, a complex is formed which we assign to Col-$(HF)_2$. The analysis of the ^1H, ^{19}F, and ^{15}N NMR signals depicted in Figures 4 and 5 indicates a zwitterionic structure of the type $[ColH]^+[FHF]^-$. The complex is fluxional and is subject to a fast exchange between two degenerate forms **1** and **2** (Figure 4). This process leads to an exchange of the two fluorine nuclei, which we label as $F_a(i)$ and $F_b(i)$ in form $i = 1,2$.

At 97 K, the ^1H spectrum consists of a broad doublet for H_b at 15.8 ppm, characterized by a coupling constant of about $^1J_{HbFb}(1) \approx 280$ Hz. The signal of H_a at 16.4 ppm exhibits two couplings, $^1J_{NHa} \approx -86$ Hz and $^1J_{HaFa}(1) \approx -75$ Hz, giving rise to a distorted triplet. The corresponding ^{19}F spectrum shows two signals, F_a and F_b at -126.2 and -166.2 ppm, which exhibit a coupling of $^2J_{FaFb} \approx 155$ Hz; the signal of F_b also exhibits the coupling $^1J_{HbFb}(1) \approx 280$ Hz. The couplings $^1J_{HbFa}(1)$ and $^1J_{NFa}(1)$ are smaller than 10 Hz and are not resolved. Both fluorine signals are coalesced at 115 K; the doublet splitting corresponds to the averages $^1J_{HbFb} = {}^1/_2[^1J_{HbFb}(1) + {}^1J_{HbFb}(2)] = {}^1J_{HbFa} = {}^1/_2[^1J_{HbFa}(1) + {}^1J_{HbFa}(2)] \approx 145$ Hz

The same splitting is observed in the signal of H_b at the same temperature (Figure 4, top), consisting of a clear triplet as expected. The couplings to H_a and N are not resolved in the ^{19}F spectrum, but $^2J_{FaFb}$ can be observed. Most remarkable is the splitting pattern of H_a at 115 K. It consists of a doublet of triplets, that is, H_a is coupled with nitrogen and both fluorine nuclei. The value of $^1J_{NHa}$ is similar to the value at 94 K. The triplets arise from coupling with both fluorine nuclei, with the average values $^1J_{HaFa} = {}^1/_2[^1J_{HaFa}(1) + {}^1J_{HaFa}(2)] = {}^1J_{HaFb} = {}^1/_2[^1J_{HaFb}(1) + {}^1J_{HaFb}(2)]$.

The superposed experimental and simulated line shapes are depicted in Figure 4; all parameters of the simulation can be retrieved from the Supporting Information. The chemical shifts are slightly dependent on temperature; however, their values do not influence the rate constants obtained. The value of the sum $^1/_2[^1J_{HbFa}(1) + {}^1J_{HbFb}(1)]$ could be extracted above 100 K from the two narrow outer components of the signal H_b; at low temperatures, $^1J_{HbFb}(1)$ could be determined directly, where $^1J_{HbFa}(1)$ is not resolved. Unfortunately, this value is too small to be extracted from the line shapes directly. However, as we observed previously a correlation between the two H−F coupling constants in FHF hydrogen bonded systems,[6d,e] we only needed to vary $^1J_{HbFb}(1)$. According to the correlation, when $^1J_{HbFb}(1)$ is of the order of $+280$ Hz, $^1J_{HbFa}(1)$ is of the order of $+10$ Hz, and this value was used throughout the simulation. The Arrhenius plot for the dynamic process is depicted in the Supporting Information. We obtain the Arrhenius parameters $A = 3 \times 10^{-13}$ s^{-1} for the pre-exponential factor and $E_a = 5$ kcal mol^{-1} for the activation energy.

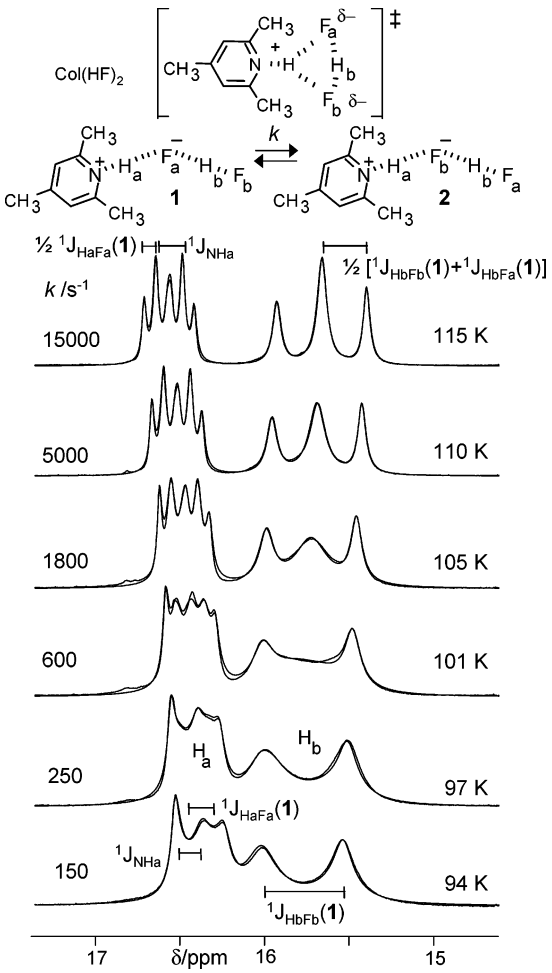

Figure 4. Superposed experimental and calculated low-temperature ^1H signals of $[ColH]^+[FHF]^-$ in CDF_3/CDF_2Cl. For further explanation, see text.

A differential line width analysis for the determination of the sign of the coupling constants reveals the following. The low-field component of the triplet of H_b is always broader than the high-field component, dominated by the positive large average $^1H-^{19}F$ coupling and an interference between dipolar and CSA relaxation. By contrast, the central line in the triplet is broader than the outer line components because the outer lines do not experience the exchange broadening, which is different from the differential transverse relaxation processes. ^1H-^{15}N coupling does not produce differential line width of the signal components of H_a, in contrast to the $^1H-^{19}F$ coupling: the high-

(18) (a) Fujiwara, F. Y.; Martin, J. S. *J. Am. Chem. Soc*. **1974**, *96*, 7625. (b) Christe, K. O.; Wilson, W. W. *J. Fluorine Chem*. **1990**, *46*, 339.

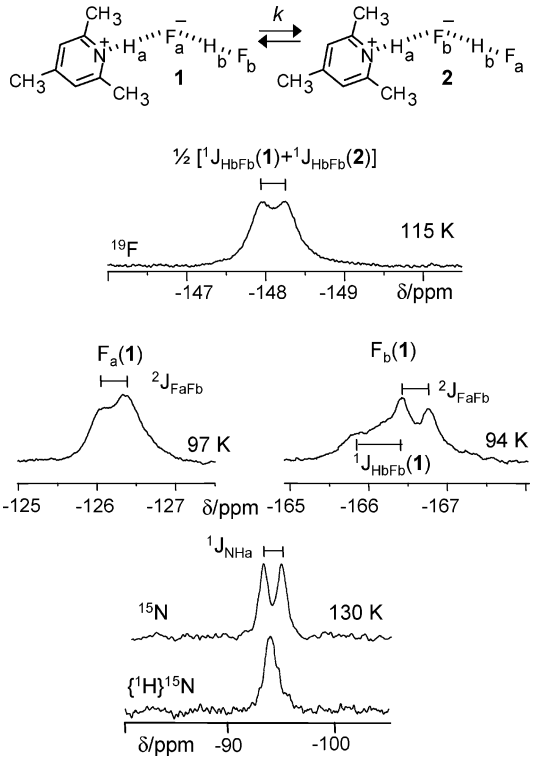

Figure 5. ^{19}F and ^{15}N signals of $[ColH]^+[FHF]^-$ in CDF_3/CDF_2Cl.

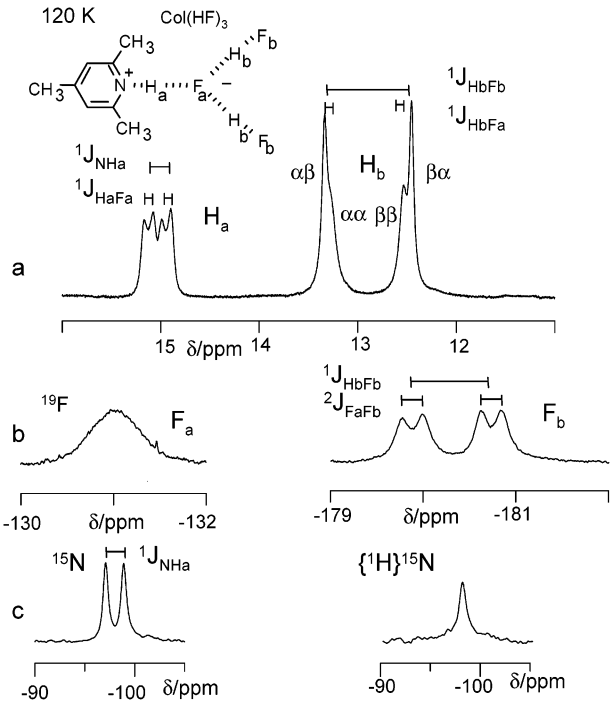

Figure 6. Low-temperature ^1H (a), ^{19}F (b), and ^{15}N (c) signals of $[ColH]^+[F(HF)_2]^-$ in CDF_3/CDF_2Cl.

field components of the triplets are again broader than the low-field components indicating a negative sign of $^1J_{HaFa}(1)$ as assumed above.

1:3 Collidine−HF Complex $[ColH]^+[F(HF)_2]^-$. The ^1H, ^{19}F, and ^{15}N signals of the 1:3 collidine−HF complex $Col(HF)_3$ are depicted in Figure 6. Two signals assigned to H_a and H_b of the intensity ratio of 1:2 are well resolved. In the ^{15}N signal a coupling to F_a cannot be resolved; however, ^{15}N is coupled to H_a with $^1J_{NHa} = -90$ Hz. The same coupling is found in the signal of H_a which is coupled in addition to F_a with $^1J_{FaHa} = -45$ Hz. We assume the negative sign because we do not think that a second sign change has occurred, although the low-field components of the $^1H-^{19}F$ doublets are again broader than the high-field components. This effect may perhaps arise from a sign change of the CSA of H_a.

H_b is split by the couplings $^1J_{FaHb} = -38$ Hz and $^1J_{FbHb} = 400$ Hz. The latter coupling reappears in the signal of F_b, where also $^2J_{FF} = 99$ Hz is resolved. F_a contributes only a broad signal, which is not surprising because of the coupling with three protons, two fluorines, and one nitrogen. These values point to a strongly asymmetric position of two protons in the F...HF fragments, like in the crystalline salt potassium dihydrogen trifluoride.[19] We note that coupling constants and chemical shifts are slightly dependent on temperature.

1:4 Collidine−HF Complex $[ColH]^+[F(HF)_3]^-$. When we added a large excess of aqueous hydrofluoric acid solution to collidine dissolved in acetone and subsequently removed water by azeotropic distillation, we obtained a white polycrystalline powder. Elemental analysis indicated the presence of a complex with the composition $Col(HF)_4$. This species showed in the low-temperature ^1H NMR spectrum a doublet at 14.02 ppm, exhibiting a coupling constant of $^1J_{NH} = -92$ Hz, similar to the peak in Figure 1c. The corresponding ^{15}N doublet peak was observed at −105.7 ppm (not shown). However, we did not manage to assign the ^1H and ^{19}F signals of the $[F(HF)_3]^-$ component of this cluster. Probably, this anion is involved in fast hydrogen bond exchange processes with other species.

Discussion

We have succeeded in characterizing by multinuclear low-temperature NMR spectroscopy novel hydrogen bonded complexes between collidine and HF. Their chemical structures which are depicted in Figure 1 are corroborated by the analysis of the scalar $^{19}F-^1H$, $^1H-^{15}N$, and $^{19}F-^{15}N$ couplings across the hydrogen bonds because the slow hydrogen bond exchange regime could be reached. These complexes not are only interesting in themselves but also present an important series of snapshots of the pathway of H from fluorine to nitrogen: in the series of NHF hydrogen bonds in ColHF, $[ColHFHCol]^+$, $Col(HF)_2$, and $Col(HF)_3$, the coupling constant $^1J_{NH}$ between ^1H and ^{15}N increases monotonically indicating a gradual displacement of the proton toward nitrogen. During this displacement, the absolute value of $^1J_{HF}$ first decreases, becomes negative, goes through a minimum, and eventually disappears. Even in the region where $^1J_{HF} \approx 0$, a large heavy atom coupling $^2J_{FN}$ is observed. A similar effect was observed previously for $^1J_{AH}$ and $^2J_{AB}$ in AHB hydrogen bonded systems such as $F^-(HF)_n$ clusters[6d] and intramolecular NHN hydrogen bonds[11d] where strong evidence for a sign change of $^1J_{AH}$ was obtained when H was shifted from A to B.

In the following, we will first discuss the properties of the individual complexes observed and then discuss correlations of the hydrogen bond NMR parameters with the hydrogen bond geometries.

Properties of Collidine−$(HF)_n$ Complexes. In the presence of an excess of collidine, the 1:1 complex ColHF dominates.

(19) (a) Mahjoub, A. R.; Leopold, D.; Seppelt, K. *Eur. J. Solid State Inorg. Chem.* **1992**, *29*, 635. (b) Chandler, W. D.; Johnson, K. E.; Campbell, J. L. E. *Inorg. Chem.* **1995**, *34*, 4943.

The NMR parameters indicate a very strong hydrogen bond, $N^{\delta+}\cdot\cdot H\cdot\cdot F^{\delta-}$, which geometry is strongly dependent on temperature. At higher temperatures, the proton is closer to F than to N, but at the lowest temperature, the proton is close to the hydrogen bond center. The reasons for temperature-dependent H-bond geometries have been discussed previously.[8,9,13] When temperature is lowered, the dielectric constant ϵ_o and hence the local electric fields are increased by solvent ordering and induce in a molecular complex A−H···B an additional dipole moment. In a first step, the induced dipole moment is created by charge transfer from B to A, leading to a displacement of H toward the hydrogen bond center and to a contraction of the A..B distance. After H has crossed the hydrogen bond center, the dipole moment is increased by increasing the A..B distance, accompanied by a further displacement of H toward B. For the complex ColHF, more quantitative conclusions can be obtained after correlating the NMR parameters with the hydrogen bond geometries.

The structure $[ColHFHCol]^+$ proposed in Figures 1 and 3 directly follows from the coupling of F with two equivalent protons and two equivalent ^{15}N nuclei. $[ColHFHCol]^+$ and $[FHF]^-$ form either a contact ion pair or a solvent separated ion pair. The reorientational mobility of $[FHF]^-$ is not substantially reduced by the cation−anion interaction. The NMR parameters are not particularly dependent on temperature. As compared to ColHF, the H-bond protons are displaced across the hydrogen bond center toward nitrogens.

Addition of another HF molecule to ColHF displaces H further toward nitrogen, that is, to a hydrogen bonded contact ion pair $[ColH]^+[FHF]^-$. The NHF hydrogen bond hinders now a free reorientation of $[FHF]^-$. The process involves the breaking of the FHN hydrogen bond, a rotation of $[FHF]^-$, and the formation of a new FHN hydrogen bond without dissociation of the complex. If the rearrangement were coupled to a dissociation, the coupling of the NH proton across the hydrogen bond to fluorine would be lost, in contrast to the experimental findings.

We note that it is normally very difficult by NMR to obtain information on the stability of a particular hydrogen bond because of the lack of reference states. Therefore, there is a tendency to take the hydrogen chemical shift as an indicator for the hydrogen bond strength. However, this approach may be valid for a series of hydrogen bonded complexes of the same type but not for complexes of different types. For example, in the complex $[ColH]^+[FHF]^-$, the proton of the FHN hydrogen bond resonates at lower field than the proton of the FHF hydrogen bond. On the other hand, the proton in the latter is more centered than in the former, and the heavy atom distance is smaller as commented already above. It is, therefore, surprising that $[FHF]^-$ is subject to the fast hydrogen bond exchange in the contact ion pair. The pre-exponential factor of the rotation, $A \approx 3 \times 10^{13}$ s^{-1}, is typical for an intramolecular reaction. The activation energy, $E_a \approx 5$ kcal mol^{-1}, is unexpectedly small. This means that the reorientation may not require a complete cleavage of the hydrogen bond and occurs, most probably, via a transition state exhibiting a bifurcated hydrogen bond. We note that Reynhardt et al.[20] observed a reorientation of FHF^- in solid $NH_4^+FHF^-$ exhibiting a similar activation energy of about 6 kcal mol^{-1}.

(20) Reynhardt, E. C.; Watton, A.; Petch, H. H. *J. Chem. Phys.* **1979**, *71*, 4421.

Scheme 1

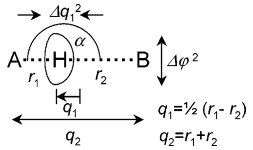

The complexes $Col(HF)_3$ and $Col(HF)_4$ can be described in terms of collidinium hydrogen bonded to the well-known anions $F^-(HF)_2$ and $F^-(HF)_3$.[6d,e] The $^1J_{NH}$ couplings are − 90 and −92 Hz, typical for protonated collidine. The exchange of the central fluorine and the terminal fluorines has become slow as compared to $Col(HF)_2$, and the FHF^- units are more asymmetric.

Hydrogen Bond Correlations. To find empirical relations between NMR chemical shifts, coupling constants, and hydrogen bond geometries in the series of collidine−HF complexes studied in this paper, we exploit geometric hydrogen bond correlations which have been established by neutron diffraction,[21] dipolar NMR, and ab initio calculations in the case of various hydrogen bonded systems.[22,23] The parameters in these correlations refer to the geometries of the "limiting structures", that is, the non-hydrogen bonded or "free" proton donors and acceptors and the configuration with the shortest heavy atom distance. These parameters have been established empirically by crystallography or computational chemistry.[22,23] In a similar way, we have proposed to construct NMR−geometry correlations using the chemical shifts or coupling constants of the limiting structures as adaptable or directly measured parameters.[5b,6,23] This approach ensures that NMR parameters reach constant values when the distances between the proton donors and acceptors are increased. A polynomial approach relating NMR parameters with hydrogen bond distances most often does not exhibit this feature; it requires the definition of the range where the polynomial approach is valid.

The geometric hydrogen bond correlations imply that the two distances r_1 and r_2 (Scheme 1) of a hydrogen bond AHB are correlated. A justification is that the sum of the empirical distance-dependent Pauling valence bond orders corresponding to these two distances is unity for the bonds from and to hydrogen.[24]

$$p_1 = \exp\{-(r_1 - r_1^\circ)/b_1\},$$
$$p_2 = \exp\{-(r_2 - r_2^\circ)/b_2\}, \text{ with } p_1 + p_2 = 1 \quad (1)$$

In eq 1, r_1° corresponds to the distance in free AH, and r_2°, to that in free HB. b_1 and b_2 can be interpreted as the parameters describing the decrease of the valence bond order with increasing distances. Instead of the average distances r_1 and r_2, we use the combinations $q_1 = {}^1/_2(r_1 - r_2)$ and $q_2 = r_1 + r_2$. In the case of linear hydrogen bonds where the average hydrogen bond angle α is about 180° (Scheme 1), q_1 corresponds to the deviation of the hydrogen nucleus from the hydrogen bond center, and q_2, to the A...B distance. Equation 1 predicts that this distance decreases when the proton is shifted from A toward the

(21) (a) Steiner, Th.; Saenger, W. *Acta Crystallogr.* **1994**, *B50*, 348. (b) Steiner, Th. *J. Chem. Soc., Chem. Commun.* **1995**, 1331. (c) Gilli, P.; Bertolasi, V.; Ferretti, V.; Gilli, G. *J. Am. Chem. Soc.* **1994**, *116*, 909. (d) Steiner, Th. *J. Phys. Chem. A* **1998**, *102*, 7041.
(22) Ramos, M.; Alkorta, I.; Elguero, J.; Golubev, N. S.; Denisov, G. S.; Benedict, H.; Limbach, H. H. *J. Phys. Chem.* **1997**, *A101*, 9791.
(23) Benedict, H.; Limbach, H. H.; Wehlan, M.; Fehlhammer, W. P.; Golubev, N. S.; Janoschek, R. *J. Am. Chem. Soc.* **1998**, *120*, 2939.
(24) (a) Pauling, L. *J. Am. Chem. Soc.* **1947**, *69*, 542. (b) Brown, I. D. *Acta Cryst.* **1992**, *B48*, 553.

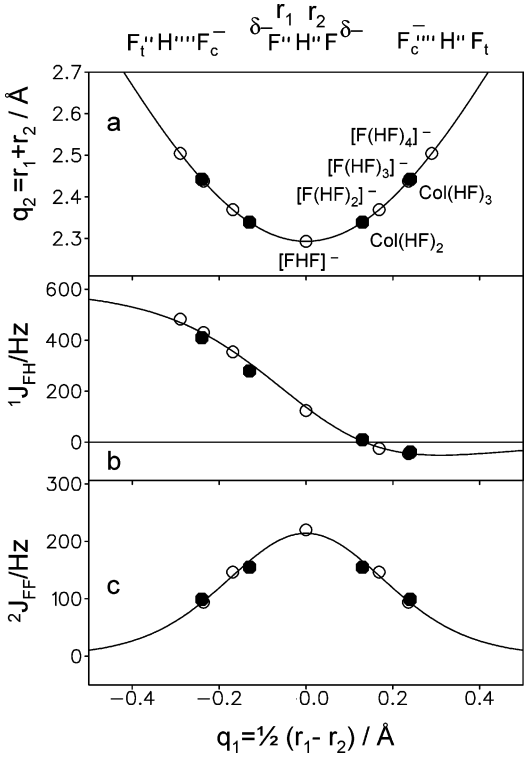

Figure 7. Hydrogen bond correlation for FHF hydrogen bonds. Plots of the F...F distance q_2 (a) and the experimental coupling constants $^1J_{FH}$ (b) and $^2J_{FF}$ (c) as a function of the hydrogen coordinate q_1 (Scheme 1). Open circles refer to $[F(HF)_n]^-$, and filled circles, to collidine−$(HF)_n$ clusters. The solid lines are calculated according to the valence bond model as described in the text.

hydrogen bond center and then increases again when the proton has crossed the center. Taking this phenomenon into account, we can determine with the parameters b_1 and b_2 together with $r_1°$ and $r_2°$ the value of the minimum A...B distance. Thus, eq 1 expands all hydrogen bond geometries in terms of the limiting structures of the free species and the strongest hydrogen bonded complex.

As has been discussed previously,[23] in the case of symmetric double well potentials or low-barrier hydrogen bonds, the average value of q_1 can be zero although q_2 has not yet reached the minimum value, and the correlation of eq 1 will be satisfied only in approximation. Also, in the case of an asymmetric strong hydrogen bond, particularly large anharmonic hydrogen zero-point vibrations visualized schematically in Scheme 1 may lead to large mean square displacements Δq_1^2 and $\Delta\varphi^2$ along the strongly anharmonic AH stretching mode and for the bending mode. These quantities may influence also the NMR chemical shifts and scalar coupling constants, an influence which is not explicitly taken into account in our treatment. However, a polynomial fit of the NMR versus geometric data will exhibit the same problem at present.

For the $[F(HF)_n]^-$ clusters, the values of r_1 and r_2 (i.e., of q_1 and q_2) had been obtained by ab initio calculations at the MP2/6-31+G(p,d) level,[6d] using the symmetries $D_{\infty h}$, C_{2v}, D_{3h}, and T_d for $n = 1-4$, in agreement with the symmetries observed by NMR. These data were used to establish the following parameters of the F−H valence bond orders in eq 1, that is, $r_1° = r_{FH}° = 0.897$ Å and $b_1 = b_{FH} = 0.36$ Å.[6e,f] For B = nitrogen, values of $r_2° = r_{HN}° = 0.992$ Å and $b_2 = b_{HN} = 0.385$ Å have been proposed.[23,24] These values were employed in the data analysis described below. To create the solid lines in Figures 7−10, first a set of data points q_1 was generated and the corresponding values of q_2 were calculated using eq 1, leading to the corresponding values of r_1 and r_2 and hence of the valence bond orders p_1 and p_2. The NMR parameters were then calculated from the latter using equations described below.

Couplings in FHF and FHN Hydrogen Bonds. The graphs of Figure 7 refer to the FHF units of $[F(HF)_n]^-$ and $Col(HF)_n$, where q_2, $^1J_{FH}$, and $^2J_{FF}$ are plotted as a function of q_1. Open circles refer to the $[F(HF)_n]^-$ clusters, and filled circles, to the complexes of collidine with HF. The solid line in Figure 7b was calculated using the following empirical equation proposed previously[6e,f] for FHF hydrogen bonds; that is

$$^1J_{FH} = {}^1J_{FH}°p_{FH} - 8\Delta J_{FHF}p_{FH}p_{HF}^2, \quad {}^1J_{FH}° = 600 \text{ Hz}, \Delta J_{FHF} = 162.5 \text{ Hz} \quad (2)$$

where $^1J_{FH}°$ is the coupling constant of hypothetical free HF dissolved in the Freon mixture. If the HF distance were increased in such a way that the valence bond order was reduced to $^1/_2$, as in $[FHF]^-$, a value of $^1J_{FH} = 300$ Hz would be obtained from the first term in eq 2. The second term in eq 2 then describes the excess decrease of $^1J_{FH}$ in $[FHF]^-$. We note that the value predicted by eq 2 for $[FHF]^-$ is 137.5 Hz, which is a little bit larger than the experimental value included in Figure 7b. A perfect fit of the experimental data would require the inclusion of additional parameters in eq 2.

The solid line in Figure 7c was calculated using the equation[6e,f]

$$^2J_{FF} = {}^2J_{FF}° 4(p_{FH}p_{HF})^2, \; {}^2J_{FF}° = 225 \text{ Hz} \quad (3)$$

The value of $^2J_{FF}°$ corresponds to the maximum value in FHF^-, calculated using CCSD ab initio methods by Perera et al.[10]

To obtain the geometries of FHF hydrogen bonds in the collidine−$(HF)_n$ complexes $[ColH]^+[FHF]^-$ and $ColHF(HF)_2$, we proceeded as follows. We varied for each complex the values of q_1 until both experimental coupling constants $^1J_{FH}$ and $^2J_{FF}$ (Table 1) fitted the solid lines of the graphs of Figure 7b and c. Then, the corresponding values of q_2 in Figure 7a were calculated using eqs 1 and 2. The estimated values of q_1 and q_2 obtained in this way are included in Table 1.

In Figure 8a, the FHN hydrogen bond correlation curve $q_2 = f(q_1)$ is plotted. The data points for the various complexes were obtained as follows. First, we rewrote eq 2 for FHN hydrogen bonds in the form

$$^1J_{FH} = {}^1J_{FH}° p_{FH} - 8\Delta J_{FHN}p_{FH}p_{HN}^2, \quad {}^1J_{FH}° = 600 \text{ Hz}, \Delta J_{FHN} = 190 \text{ Hz} \quad (4)$$

where the parameter $^1J_{FH}°$ referring to free HF is the same as in eq 2. The parameter ΔJ_{FHN} needed to be adapted and represents again the difference between $^1J_{FH}$ for the strongest FHN−hydrogen bond with $p_{FH} = p_{HN} = ^1/_2$ and the diatomic molecule FH with a bond length corresponding to a valence bond order $p_{FH} = ^1/_2$.

We noticed that the values of $^1J_{FH}$ exhibit a minimum around −75 Hz (Table 1), whereas the values of $^1J_{HN}$ decrease monotonically. By setting the parameter ΔJ_{FHN} to a value of 190 Hz, we were able to reproduce this minimum value using

Table 2. Primary Isotope Chemical Shift Effect $^{p}\Delta$(D/H) ≡ $\delta(F^2HN) - \delta(F^1HN)$ in the NHF Hydrogen Bond of the Collidine−HF Complex in CDF_3/CDF_2Cl

species	$^{p}\Delta$(D/H)/ppm[a]	ϵ_0[a,b]	T/K [a]	r_{NH}/Å	r_{HF}/Å	q_1/Å	q_2/Å
ColHF	−0.20	13.5	190	1.26	1.15	−0.05	2.41
ColHF	0.16	16.1	170	1.23	1.18	−0.02	2.41
ColHF	0.27	20.4	145	1.20	1.21	0	2.41
ColHF	0.26	24.5	145	1.19	1.22	0.02	2.42
ColHF	0.23	26.1	135	1.19	1.23	0.02	2.42
ColHF	0.21	25.4	125	1.20	1.21	0	2.41
ColHF	0.20	28.9	130	1.18	1.24	0.03	2.42
ColHF	0.20	28.6	125	1.19	1.23	0.02	2.42
ColHF	0.19	30.0	125	1.19	1.23	0.02	2.42
ColHF	0.18	30.3	110	1.16	1.27	0.05	2.43
ColHF	0.10	37.7	103	1.17	1.26	0.04	2.43

[a] Data taken from ref 8. [b] Dielectric constant of the CDF_3/CDF_2Cl mixture is a function of temperature and solvent composition.

eq 4, leading to the solid line of Figure 8b. In the next step, we varied the values of q_1 for all data points of Table 1 in such a way that eq 4 was fulfilled for all $^1J_{FH}$ values. The value of ColHFHCol was placed on the left side, and the values of ColHFHF and ColHF$(HF)_2$, on the right side of the minimum taking into account the large negative values of $^1J_{HN}$ of the latter two complexes. Having obtained the q_1 values of all data points (Table 1), we could determine the values of q_2 depicted in Figure 8a using the NHF−hydrogen bond correlation (Table 1). In the next steps, we plotted in Figure 8c and d the experimental values of $^1J_{HN}$ and of $^2J_{FN}$ as a function of q_1 and determined the parameters of the corresponding correlation curves by adapting the parameters in the equations

$$^1J_{HN} = {}^1J_{HN}^{\circ}\, p_{HN} - 8\Delta J_{NHF} p_{FH} p_{HN}^2, \quad {}^1J_{HN}^{\circ} = -100 \text{ Hz}, \Delta J_{NHF} = 12.5 \text{ Hz} \quad (5)$$

$$^2J_{FN} = {}^2J_{FN}^{\circ}\, 4(p_{FH}p_{HN})^2, \; {}^2J_{FN}^{\circ} = 97.5 \text{ Hz} \quad (6)$$

The results are indicated by the solid lines, and the fit is quite satisfactory.

Let us come back to the effects of the changes of the hydrogen bond geometries of ColHF in CDF_3/CDF_2Cl in the temperature range between 200 and 100 K. In this temperature range, the dielectric constant ϵ_o of a 1:1 solvent mixture increases from about 15 to 45;[8] these values depend also on the composition of the solvent mixture. As was discussed before,[8] the dielectric constant increase leads for ColHF to a displacement of the proton from F toward N, but this displacement could not be quantified. In the same dielectric constant range, a sign change of the primary isotope chemical shift effect $^{p}\Delta$(D/H) ≡ $\delta(F^2HN) - \delta(F^1HN)$ was observed,[8] indicating that at low temperatures a quasi-single well potential is reached where D is confined more to the hydrogen bond center as compared to H. By contrast, at higher temperatures, D is located closer to F in comparison to H.

As Figure 8 provides a calibration of the NMR parameters in terms of hydrogen bond geometries, we are now able to quantify the solvent induced geometric changes of ColHF. According to Tables 1 and 2 and Figure 8a, the increase of ϵ_o from 13.5 to 37.7 leads for ColHF to an increase of the F−H bond length from 1.15 Å to about 1.3 Å and to a decrease of the N−H bond length from 1.26 Å to about 1.15 Å. At values of ϵ_o between 20 and 25, the proton is almost located in the hydrogen bond center, with two similar FH and NH distances

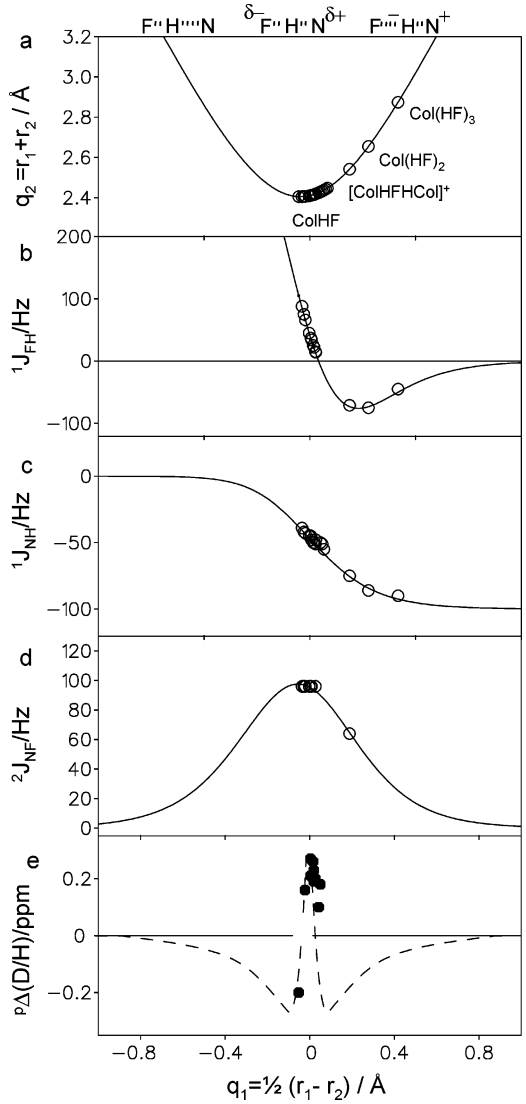

Figure 8. Hydrogen bond correlation for FHN hydrogen bonds q_2 as a function of q_1 (a). Plot of the experimental coupling constants $^1J_{FH}$ (b), $^1J_{HN}$ (c), and $^2J_{FN}$ (d) and the primary isotope chemical shift effect $^{p}\Delta$(D/H) (e) as a function of q_1. The solid lines are calculated according to the valence bond model as described in the text.

of 1.2 Å (Table 2). During the proton displacement the N..F distance remains fairly constant around 2.42 Å which is in agreement with the finding that the coupling constant $^2J_{FN}$ also remains constant.

The changes of the primary isotope chemical shifts $^{p}\Delta$(D/H) as a function of q_1 are depicted in Figure 8e. Unfortunately, only a small part of this dependence was accessible experimentally. Therefore, we were not able to derive an empirical equation for this dependence but added the dotted line as a guide for the eye, where the shape of the curve was adopted from calculations published previously for other strong hydrogen bonded systems.[23] Nevertheless, it is clear that the positive part of $^{p}\Delta$(D/H) is restricted to a very narrow region of the geometric hydrogen bond correlation and points such as an arrow to the region where one assumes a quasi-symmetric single well potential for the proton stretching motion in hydrogen bonds.

Chemical Shifts of FHF and FHN Hydrogen Bonds. In this section, we will use the valence bond order model to describe the chemical shift of nuclei in a hydrogen bond AHB

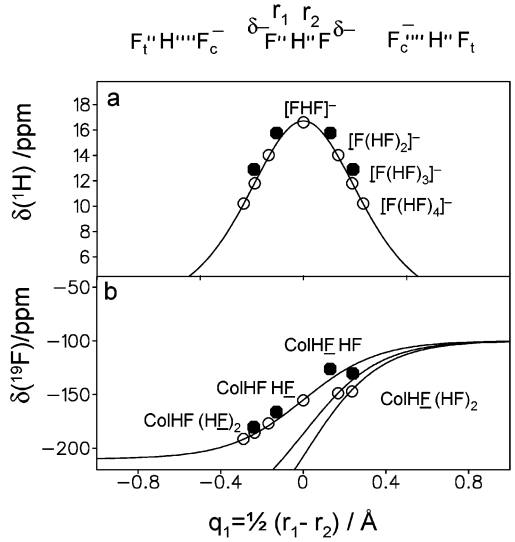

Figure 9. ^{1}H (a) and ^{19}F (b) chemical shifts of the FHF hydrogen bonds of $[F(HF)_n]^-$ (open circles) and collidine−$(HF)_n$ clusters (filled circles) as a function of q_1. The solid lines are calculated according to the valence bond model as described in the text.

in terms of the following equation

$$\delta_i = p_{AH}\delta_i(AH)^\circ + p_{HB}\delta_i(HB)^\circ + 2^k 2^l \Delta\delta_i(AHB) p_{AH}{}^k p_{HB}{}^l \quad (7)$$

We had already used this equation in order to describe the chemical shifts of the proton, but we realize here that it can also be used for the heavy atoms. k and l are parameters which need to be adapted. $\delta_i(AH)^\circ$ and $\delta_i(HB)^\circ$ are the limiting chemical shifts of nucleus i in the "free" residues AH and HB. $\Delta\delta_i(AHB)$ describes the deviation of the chemical shift of nucleus i from the average value $^1/_2(\delta_i(AH)^\circ + \delta_i(HB)^\circ)$ when the valence bond orders are both $^1/_2$, corresponding in the case of A = B to the strongest symmetric "proton shared" hydrogen bond. $\Delta\delta_i(AHB)$ will depend not only on both the chemistry, that is, the type of A and B, and their chemical surroundings but also on the A...B distance in the symmetric complex. A problem with the use of the above equations is that the limiting chemical shifts $\delta_i(AH)^\circ$ and $\delta_i(HB)^\circ$ refer to the fictitious limiting structures which cannot easily be determined experimentally. By contrast, the limiting coupling constants across an infinitely long hydrogen bond are zero by definition.

^{1}H Chemical Shifts. In Figures 9 and 10, we have plotted the ^{1}H, ^{19}F, and ^{15}N NMR chemical shifts of the FHF and NHF hydrogen bonds of the species studied as a function of the values of q_1 determined in the previous section. In Figure 9a are depicted the ^{1}H chemical shifts of the hydrogen bonds in the FHF fragments. We note that the parameter $\delta_H(FH)^\circ$ in eq 7, the ^{1}H chemical shift in the FH monomer, is of the order of 2 ppm. In this case, the suitable data set in eq 7 is $l = k = 2$ and $\Delta\delta_H(FHF) = 14.7$ ppm.[6f]

The ^{1}H chemical shifts of the FHN hydrogen bond are illustrated in Figure 10a. The solid line was calculated using

$$\delta H = p_{FH}\delta_H(FH)^\circ + p_{HN}\delta_H(HN)^\circ + 8\Delta\delta_H(FHN) p_{FH} p_{HN}{}^2 \quad (8)$$

with $\delta_H(FH)^\circ = 7.7$ ppm, $\delta_H(HN)^\circ = 7$ ppm, and $\Delta\delta_H(FHN)$ = 11 ppm. The latter value was taken from the limiting collidinium value in the collidine−carboxylic acid series of ref 5b.

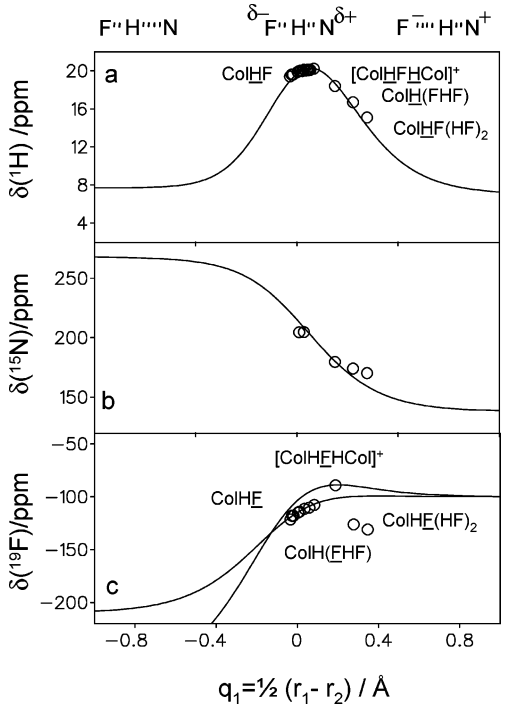

Figure 10. ^{1}H (a), ^{15}N (b), and ^{19}F (c) chemical shifts of the FHN hydrogen bonds of collidine−$(HF)_n$ clusters as a function of q_1. The solid lines are calculated according to the valence bond model as described in the text.

^{15}N Chemical Shifts. The dependence of the ^{15}N chemical shifts of the FHN hydrogen bonds on q_1 is illustrated in Figure 10b. The solid line corresponds to the equation

$$\delta_N = \delta_N{}^\infty p_{FH} + \delta_{NH}{}^\circ p_{HN} + p_{FH} p_{HN} \Delta\delta_N(FHN) \quad (9)$$

with $\Delta\delta_N(FHN) = 90$ ppm, $\delta_N{}^\infty = 268$ ppm, and $\delta_{NH}{}^\circ = 138$ ppm. The latter two values were measured previously for free collidine and for collidinium,[5b] using $^{15}NH_4Cl$ as reference. Thus, only $\Delta\delta_N(FHN)$ needed to be adapted.

^{19}F Chemical Shifts. We come now to the discussion of the fluorine chemical shifts of the investigated complexes. In Figure 9b are depicted the ^{19}F chemical shifts of the FHF hydrogen bonds, of both the $[F(HF)_n]^-$ clusters (open circles) analyzed previously[6e] and the new data points for $Col(HF)_2$ and $Col(HF)_3$ (closed circles). The data points with negative values of q_1 correspond to terminal fluorines, whereas those with positive values, to central fluorines. The latter are involved in two or three hydrogen bonds and need, therefore, a different treatment than the terminal fluorines which are involved only in a single bond as it is shown by the three different curves.

The solid lines were calculated using the equation

$$\delta_F = r\delta_{FH}{}^\circ p_{FH} + \delta_F{}^\infty p_{HF} \quad (10)$$

with $\delta_F{}^\infty = -100$ ppm and $\delta_{FH}{}^\circ = -210$ ppm determined previously for $[F(HF)_n]^-$ [6e] and $r = 1$ for the terminal fluorines and for $[FHF]^-$. The values $r = 1.3$ and 1.5 were adapted in order to fit the chemical shifts of the central fluorines in $[F(HF)_2]^-$ and $[F(HF)_3]^-$.

We note that the new data points of $[ColH]^+[FHF]^-$ and $[ColH]^+[F(HF)_2]^-$ are located only slightly above the line calculated for $[FHF]^-$ and for $[F(HF)_2]^-$. In other words, the chemical shifts of the central fluorines in these clusters are almost determined by the hydrogen bond to HF rather than to collidinium. This result is not surprising, as the q_1 values of the FHF bonds are substantially smaller than those of the FHN hydrogen bond; that is, the distance of the central fluorine to the H in the FHF hydrogen bond is smaller than that to H in the FHN hydrogen bond.

We come now to the fluorine chemical shifts of the FHN hydrogen bonds. The data points are depicted in Figure 10c. The solid line was calculated using the equation

$$\delta_F = \delta_{FH}{}^{\circ} p_{FH} + \delta_F{}^{\infty} p_{HN} + s p_{FH} p_{HN} \Delta\delta_F(\mathrm{FHN}) \quad (11)$$

where $s = 1$ for the single FHN hydrogen bonds and $s = 1.5$ for the fluorine with two FHN hydrogen bonds, $\Delta\delta_F(\mathrm{FHN}) = 150$ ppm, and the same parameters $\delta_F{}^{\infty} = -100$ ppm and $\delta_{FH}{}^{\circ} = -210$ ppm as those for the FHF hydrogen bonds. Thus, the fluorine chemical shifts in "free" HF and F^- are independent of the reaction partner F^- or collidine. However, while the q_1 value of $[FHF]^-$ is zero and that of ColHF is close to zero, the chemical shifts of the fluorines in both complexes are very different (Table 1), that is, -155 and -115 ppm. The latter value is almost already close to the value $\delta_F{}^{\infty}$ of "free" fluoride. These differences are taken into account by the term $\Delta\delta_F(\mathrm{FHN})$. The consequence is that once the proton has crossed the hydrogen bond center, the fluorine chemical shifts do not change anymore.

It is understandable that we need the term $\Delta\delta_F(\mathrm{FHN})$: a look at Figures 7a and 8a shows that the shortest F...F distance in $[FHF]^-$ is about 2.3 Å whereas the shortest F...N distance is 2.4 Å. Thus, a fluorine in the shortest FHN hydrogen bond resonates at lower field than in the shortest FHF hydrogen bond. Naturally, a detailed quantum-mechanical study would reveal effects arising from electronic differences of fluorine and nitrogen. The data point of $[ColHFHCol]^+$ was accommodated by a different value of $\Delta\delta_F(\mathrm{FHN})$. We note that the chemical shift of this fluorine is very low-field, even lower than that of "free" fluoride.

Finally, in Figure 10c are also included the chemical shift values of the central fluorine in $[ColH]^+[FHF]^-$ and $[ColH]^+[F(HF)_2]^-$, where the value of q_1 is defined for the FHN hydrogen bond. Naturally, these data points cannot fit the calculated lines because the contribution of the FHF bond determines these chemical shifts as discussed above.

Conclusions

We have succeeded in measuring and analyzing the chemical shifts and scalar coupling constants across hydrogen bonds of a series of novel collidine$-(HF)_n$ complexes in CDF_3/CDF_2Cl mixtures, exhibiting a high polarity at low temperatures. This series represents a model system where the effects of proton transfer from F to N and from F to F on the NMR parameters can be studied. The dependence of the NMR parameters can be well described in terms of the valence bond order−hydrogen bond correlation model.

Acknowledgment. This work has been supported by the Deutsche Forschungsgemeinschaft, the Russian Foundation for Basic Research, Grant 03-03-32272, and the Fonds der Chemischen Industrie, Frankfurt.

Note Added in Proof. J. Del Bene et al.[25] have performed high quality ab initio EOM-CCSD calculations of the coupling constants J_{FH}, J_{HN}, and J_{FN} of the 1:1 complexes FH···NH_3 and FH···pyridine as a function of the F...H and F...N distances. They found that the values of $|J_{FH}|$ decreased and that of $|J_{HN}|$ increased in the region of the strong F··H··N hydrogen bond, whereas $^2J_{FN}$ remained constant, in very good agreement with the experimental NMR data reported recently[8,13] and in this paper.

Supporting Information Available: A detailed description of the simulation of the spectra of Figure 5 and further information. This material is available free of charge via the Internet at http://pubs.acs.org.

JA029183A

(25) Del Bene, J. E.; Bartlett, R. J.; Elguero, J. *Magn. Reson. Chem.* **2002**, *40*, 767.